Vibrational Spectroscopic [FT-IR, FT-RAMAN] Investigation on Sulphanilamide Using Computational [HF And DFT] Analysis

Ms.S.Subasri[1], Mrs.T.Aarthi[2], Ms.G.Bairavi[3]
[1]Dept of Physics
[2] Assistant Professor and HOD, Department of Science & Humanities
[3] Assistant Professor and HOD, Department of Civil Engineering
[1]Government Arts college, Mannarkudi,
[2, 3]SRVEC

Abstract- *A recently identified new organic nonlinear optical (NLO) material, 3-Aminopyridine 4-Nitrophenol (3AP4NP) was synthesized and good quality single crystals were grown by slow evaporation solution growth technique. Microanalysis, powder XRD and FT-IR spectral studies were performed on 3AP4NP to ascertain its composition, phase and various characteristic functional groups respectively. The NLO efficiency was measured to be about 2.7 times greater than that of standard KDP. The UV-Vis-NIR and fluorescence spectral data of the crystal were recorded to explore its optical transmission and emission properties respectively. The dielectric properties were evaluated as a function of frequency at various temperatures.The hardness test performed at room temperature revealed the moderate hardness of the material. Quantum chemical calculations were performed for the title molecule by DFT using B3LYP/6-311 + + G (d,p) basis set to analyze first hyperpolarizability, HOMO–LUMO energies and molecular electrostatic potential.*

Keywords- Diffractometry (XRD) Xeleratordetecter, NIR spectrophotometer .

I. INTRODUCTION

In recent years, extensive researches are being carried out worldwide to synthesize new compounds and grow single crystals with non-centro symmetric space group as they possess highly aligned and stable dipolar NLO chromophores along with certain desired physico-chemical properties such as higher NLO and large electro optic coefficients, small dielectric constant (hence faster response), ease of synthesizing new molecules due to inherent flexibility, higher laser damage threshold for laser power (>10 GW/cm^2), possible integration into devices to realize their applications in the fields such as optical communication, Terahertz wave technology, etc .

II. EXPERIMENTAL DETAILS

MATERIAL SYNTHESIS AND CRYSTAL GROWTH

All chemicals and reagents used for the synthesis were of analytical grade (purity ≥98%), procured from Merck, India and used as received without any further purification. The calculated amount of the starting materials (3-Aminopyridine and 4-Nitophenol) taken in 1:1 molar ratio dissolved separately in ethanol were thoroughly mixed and stirred well continuously for 6 h using a motorized magnetic stirrer to prepare a homogeneous mixture of the solution. The yellow crystalline precipitate that settled at the bottom of beaker was separated, washed with ethanol and then dried in a hot air oven to obtain the stable yellow microcrystalline powder. The material thus synthesized was re-crystallized two or three times in ethanol to enhance the purity and the final product was kept in an airtight pack which was then utilized for further growth. The reaction scheme is involved in the chemical synthesis of the title compound.

The solubility of 3AP4NP was analyzed in methanol, ethanol, acetone, acetonitrile and toluene however mixed solvent of toluene and ethanol (1:3) was found to possess moderate solubility suitable for the controlled growth of 3AP4NP. A saturated solution of the title compound was prepared at room temperature (≈30 °C) by dissolving the purified starting material in the mixed solvent of toluene and ethanol (1:3) and the clear solution obtained after complete dissolution of the starting material was filtered twice using a Whattman filter paper (grade No. 1) to remove the suspended residual solutes and impurities if any, into a clean dry crystallizer. The filtrate collected in the crystallizer was tightly covered with a thin polythene sheet with an optimally perforated lid at the top and kept in the water bath for controlled evaporation of the solvent. After a period of 1 month, spontaneous nucleation was observed in the solution and subsequently optically transparent and yellow colored,

good quality single crystal having the dimension of 7 mm × 4 mm × 1 mm was collected from the mother solution using a well-cleaned forceps. The grown crystal was found to be chemically stable and non-hygroscopic with well facetted morphology at ambient temperature (Fig. 1).

III. CHARACTERIZATION TECHNIQUES

INTRODUCTION

The prepared undoped and doped ZnO films on glass substrates have been systematically analyzed to identify their structural, morphological and optical properties. In this chapter, the characterization techniques, instruments used for these studies are briefly explained. Simultaneously, the instrumental details and the experimental procedures that have been adopted to carry out these studies are elaborated.

IV. THICKNESS MEASUREMENT BY NON-DESTRUCTIVE STYLUS METHOD

The surftest SJ-301 is a stylus type surface roughness and thickness measuring instrument. It can be used to measure the thickness by forming a step height on any uniform surface. The instrument is self explanatory. The stylus of the SJ-301 detector unit traces the minute irregularities of the coating surface. Surface roughness is determined from the vertical displacement produced during the detector traversing over the surface irregularities.

When the thickness is to be measured, the stylus is placed over the uncoated surface and made to move towards the coating. Then it steps over the coating and moves over the coating surface for some distance. There is an upward shift in the trace near the stylus. The vertical displacement gives the thickness of the coating. The measurement results are displayed digitally/graphically in μm on the tour panel. The thicknesses of all the ZnO coatings are found using this instrument. It is a non-destructive technique and the coating may be used for further studies without any damage.

V. STRUCTURAL CHARACTERIZATION

X-ray diffractometry (XRD) is a powerful non-destructive diagnostic tool in analyzing the crystalline phases of the material and determining the structural properties of these phases such as the preferred orientation and average crystallite size. The XRD gives inter-planar spacing, which is used for identification of different phases and corresponding structure of the material present in the studied resistive sensors..

When an X-ray beam falls on matter, scattered X-radiation is producedX-ray diffractometry (XRD) is a powerful non-destructive diagnostic tool in analyzing the crystalline phases of the material and determining the structural properties of these phases such as the preferred orientation and average crystallite size. The XRD gives inter-planar spacing, which is used for identification of different phases and corresponding structure of the material present in the studied resistive sensors by all the atoms. These scattered waves spread out spherically from all the atoms in the sample, and the interference effects of the scattered radiation from different atoms cause the intensity of the scattered radiation, to exhibit maxima and minima in various directions. The equipment consists of a X-ray generator, diffractometer, proportional counter and single channel pulse height analyzer. The specimen is mounted in the center of the diffractometer and rotated by an angle around an axis in the film plane. The counter is attached to an arm rotating around the same axis by angle (2θ). It can be observed that the diameter of the focusing circle continuously shrinks with increasing diffraction angle. Only (hkl) planes parallel to the film contributes to the diffracted intensity.

The X-ray diffraction patterns of all films were recorded by using the following configuration based X-ray diffractometer. In the present work, X-ray diffraction studies were carried out on ZnO, MZO and AZO thin films at different annealing temperatures. The technical details of the X-ray diffractometer used in the present study are:

Model : PANalyticalX'Pert ProX-ray source:1.8 kW ceramic copper tube
Operation potential : 40 kV, 30 mA
Filter : Nickel
Radiation used: CuK_{α} - 1.54056 Å
Detector : Xeleratordetecter

The obtained diffraction peaks were indexed with standard JCPDS cards and evaluated the various crystalline parameters like, lattice constants, crystallite size and crystalline phase of the films.

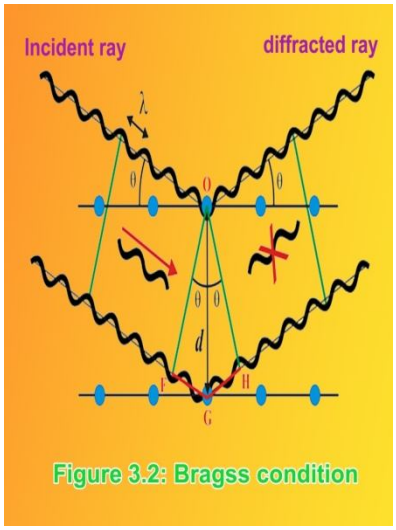

VI. OPTICAL CHARACTERIZATION

UV-VIS-NIR SPECTROPHOTOMETER

Atoms, molecules and complex ions absorb radiation of different wavelengths. An absorption spectrum will show a number of absorption bands corresponding to structural groups within the atoms, molecule and complex ions. Many molecules absorb ultraviolet or visible light.

Optical properties are of much importance for thin films. The measurement of transmission or reflection of a sample provides a satisfactory way to determine the form of the absorption edge. The absorption edge and energy band gap can be determined from the transmission measurement. The UV-visible absorption data of undoped and doped ZnO thin films having different annealing temperature (350 ^{o}C-450 $^{\circ}$C) were recorded using Hitachi 3400 UV-Vis-NIR spectrophotometer. The optical measurements at normal incidence were carried out in the range of 200-800 nm.

When the light is incident on a thin film material with energy equal or greater than that of the band gap, absorption of the photons can take place and electrons can jump from valence band to the conduction band, creating electron hole pairs. The material absorbs little and can transmit the photons having energy less than the band gap of the semiconductors, as the energy is insufficient to create an electron hole pair. The ability of a material to absorb photons of a given wavelength is measured quantitatively by the optical absorption coefficient (α), measured in units of reciprocal distance.

There are two major types of intrinsic absorption processes involved in determining α, they are the direct and indirect absorption. As a general rule, the larger the band gap, the smaller is the value of α for a given wavelength but absorption coefficient also depends on the density of states in the conduction and valence bands. The optical absorption coefficient is related with the energy band gap and it is given by the following equation [3]:

$$\alpha h\upsilon = B\,(h\upsilon - E_g)^n$$

Where B is a constant, E_g is optical band gap and n is the exponent. For crystalline semiconductors, n is ½, 3/2, 2 and 3 when the transition is direct allowed, direct forbidden, indirect allowed and indirect forbidden, respectively. Apparently the plot of $(\alpha h\upsilon)^2$ or $(\alpha h\upsilon)^{1/2}$ against $(h\upsilon)$ provides the nature and E_g value of a particular film.

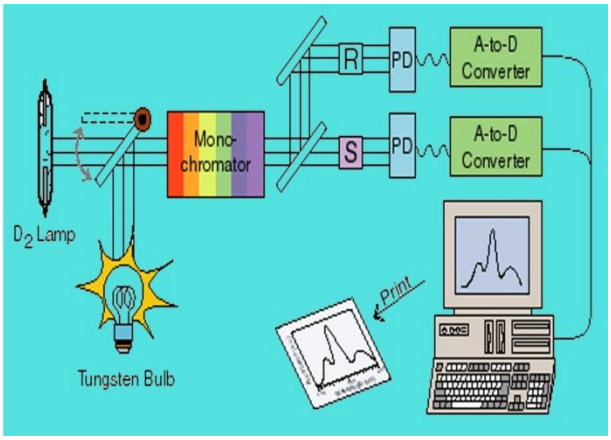

VII. RESULTS AND DISCUSSIONS

MICROANALYSIS AND POWDER XRD STUDIES

The results of CHN analysis revealed that the percentage composition of Carbon, Hydrogen and Nitrogen were respectively 77.68% (77.16%), 7.01% (6.48%) and 15.08% (16.36%) and they agreed well with those obtained from theoretical values that are provided in the parenthesis. This study shows that the synthesized compound is free from impurities which in-turn confirmed the formation of the complex in the stoichiometric proportion. From the powder X-ray diffraction data, various planes of reflections were indexed using Mercury software. The observed d values for different angles of incidence (2θ) with their corresponding (hkl) indices of 3AP4NP were given in Table1. The indexed powder X-ray diffraction pattern (Fig.2) was compared with the XRD pattern simulated by the Mercury software and was found to agree with each other which confirmed the grown crystal is indeed 3AP4NP.

OPTIMIZED GEOMETRY

The optimized molecular structure of 3AP4NP with atom numbering scheme obtained from GAUSSIAN 03 and

GAUSS VIEW programs is shown in Fig. 3. The most optimized structural parameters such as bond length, bond angle and dihedral angle obtained by B3LYP/6-311 + + G(d,p) level in accordance with the atom numbering scheme were summarized in Table2 and compared with the experimental single crystal XRD data of the similar compound reported previously by Draguta et al. In the assessment of bond lengths it could be observed that most of the theoretically predicted values are slightly greater than the experimental values. The main reason for this minor discrepancy observed in the structural parameters obtained by theoretical and experimental methods could be attributed to the isolated 3AP4NP molecule and the three dimensional crystalline solid. The bond angles and dihedral angles calculated using B3LYP/6-311 + + G (d,p) level also showed the same trend as the variation in the bond length.

FT-IR SPECTRAL STUDIES

In vibrational spectroscopy, identification of various functional groups present in the crystal is achieved by inspecting the primary absorption spectral bands appearing in the recorded spectrum since they could be often associated with particular functional groups. Figure4 shows the recorded FT-IR spectrum of the title compound wherein the observed absorption peaks and their corresponding vibrational assignments, compared with standard spectra of the functional groups, are tabulated (Table3). In the present study, a weak band that appears at 3082 cm^{-1} has been assigned to aromatic C–H stretching vibration. The intense sharp peaks identified at 1289, 1170, 1104 cm^{-1} were endorsed to C–H in-plane bending and the medium intensity peaks observed at 846, 796, 751, 690 cm^{-1} confirmed C–H out-of-plane bending vibrations. The weak absorption noticed at 1331 cm^{-1} indicates aromatic C–C stretching vibration whereas the two medium strong bands seen at 1587 and 1491 cm^{-1} could be attributed to aromatic C=C stretching vibration. As C–C in-plane bending vibrations is expected to occur in the region 1000–675 cm^{-1}, the medium intensity bands detected at 846, 796, 751, 690 cm^{-1} could be attributed to this stretching mode. The medium strong band appeared at 3477, 3374 and 3220 cm^{-1} could be assigned to hydroxyl (O-H) stretching vibrations. As O-H in-plane bending is supposed to occur in the range 1250–1150 cm^{-1} the band observed at 1170 cm^{-1} could be attributed to this stretching mode. In aromatic compounds, the identification of C–N and C=N stretching vibrations is relatively a difficult task since mixing of several bands is possible in this region. The weak and medium strong absorption identified respectively at 1331, 1289 and 1587 cm^{-1} were characteristic of aromatic C–N stretching and C=N stretching vibrations. Further the strong band predicted at 640 cm^{-1} corresponds to C–N in-plane bending vibration and the weak band viewed at 690 cm^{-1} could be due to the effect of C–C–N in-plane stretching mode which is also assigned to N-H out of plane bending vibration. The asymmetric and symmetric modes of NH_2 group were assigned to 3477 and 3374, 3220 cm^{-1}. A very strong band found at 1587 cm^{-1}has been designated to NH_2 scissoring mode and the weak bands observed at 1104 cm^{-1} could be ascribed to NH_2 rocking mode. The absorption bands appear at 1491 and 1331 cm^{-1} were assigned to the asymmetric and symmetric stretching modes of NO_2 groups. As almost all the absorption peaks observed in the recorded spectrum were assigned by the expected functional groups of the title compound, it could be stated that the presence of impurities was below the detectable limit and thus the recorded FT-IR spectrum strongly confirmed the formation of the title compound.

NLO STUDIES

By employing the Kurtz-Perry powder technique, the SHG signal output for 3AP4NP crystalline powder was found to be about 150 mV whereas for standard KDP powder it was about 55 mV. The obtained SHG efficiency of 3AP4NP powder was found to be 2.72 times greater than that of the standard KDP. Comparative SHG efficiency of 3AP4NP crystal along with other well-known pyridine group of organic NLO crystals with respect to KDP were summarized in Table4.

THERMAL STUDIES

Figure a, b showed respectively the simultaneously recorded TG/DTA and DSC thermograms for 3AP4NP crystal from which the thermal stability, decomposition temperature and phase transition could be explained. DTA trace reveals that 3AP4NP crystal undergoes an irreversible endothermic transition at 96.55 °C which signifies the onset of melting and the endothermic dip at 102.57 °C where the melting terminates corresponding to its melting point. The sharpness of the endothermic dip ensures purity and good degree of crystallinity of the grown crystal. However no significant weight loss has been observed in TG curve. From TG trace, it could be observed that the crystal was thermally stable upto 150.21 °C without any decomposition since no appreciable weight loss was noticed below this temperature especially around 100 °C which confirmed the absence of the crystallization solvent or impurity in the crystal lattice.

On further heating TG curve showed a small weight loss indicating the process of decomposition subsequently followed by a complete weight loss of about 100% in a single step from 150.21 °C (6.2977 mg) to 237.07 °C with 0 mg as

residue taking away all fragments of the title compound as volatile gaseous product leading to massive decomposition. The sharp endothermic peak (T peak) at 102.57 °C with enthalpy change (ΔH) 175.9 J/g in the DSC trace represent solid–liquid phase transition which corresponds to the melting of 3AP4NP and this agrees with those observations found in TG/DTA measurement. Hence the grown crystal of 3AP4NP could be used for any applications below 96.55 °C.

OPTICAL STUDIES

NLO material can be of practical use only, if it has lower cut-off below 400 nm and wide optical transmission window withsout any absorption at the fundamental and second harmonic wavelengths since absorptions, if any, near the fundamental or second harmonic will lead to the loss of conversion efficiency in those wavelengths. Figure 6a shows the optical transmission spectrum in the UV-VIS–NIR region with no appreciable absorption of light observed in the region between 298 and 1107 nm, which leads to modest optical transmission window with the maximum optical transparency of about 50% in the entire visible region. The lower cutoff wavelength was found to occur at 298 nm, due to promotion of an electron from a non-bonding (lone-pair) 'n' orbital to an antibonding 'π' orbital designated as π* (n → π*). The lower-cut off wavelength combined with meek optical transparency in the VIS–NIR region is suitable for the generation of second harmonic waves (532 nm) as well as third harmonic wave light (354.6 nm) from the Nd: YAG laser of wavelength 1064 nm [36]. The optical band-gap energy (E_g) of the as grown crystal in the lower cut-off wavelength region (298 nm) was calculated to be 4.161 eV using the theoretical formula,
UV-Vis–NIR spectrum of 3AP4NP single crystal **a** Optical transmission, **b** Tauc's plot of (αhν)1/2(αhν)1/2versus photon energy (hν)(hν) Eg=(1240λ) eVEg=(1240λ) Ev

where λ is the lower cut off wavelength (298 nm). The measured transmittance (T) canbe used to calculate the absorption co-efficient (α) using the relation =2.3026 log(1T)t=2.3026 log(1T)t

where 'T' is the percentage of transmittance and 't' is the thickness of the crystal

The optical band-gap (E_g) was evaluated from the transmission spectrum and the optical absorption co-efficient (α) near the absorption edge is given by
(αhν)n=A(Eg−hν)(αhν)n=A(Eg−hν)

where 'A' is a constant, 'E_g' the optical band-gap, 'h' Planck's constant and 'ν' the frequency of the incident photon. The band-gap energy (E_g) of the 3AP4NP single crystal (inset of Fig. 6b) was, estimated from UV–Vis transmittance data using the Tauc's plot of $(\alpha h\nu)^{1/2}$ versus incident photon energy (hν) by extrapolating the linear portion of the curve to a point $(\alpha h\nu)^{1/2} = 0$ and it was found to be 4.187 eV, which is ingood agreement with the theoretical value of 4.161 eV.

VIII.CONCLUSION

In this work, a detailed account of 3AP4NP, which is identified as a suitable organic NLO crystal, has been provided. Single crystals of 3AP4NP were grown by slow evaporation technique and it was confirmed to crystallize in monoclinic crystal system with non-centro symmetric space group.The composition, crystalline phase and functional groups were confirmed by CHN, Powder XRD and FT-IR analyses respectively. The powder SHG efficiency was confirmed by Kurtz-Perry powder technique and found to be about 2.7 times greater than that of the standard KDP.

IX. ACKNOWLEDGEMENT

We Thankful to Dr.G.M.BALAMURUGAN, Principal of Sembodai Rukmani Varatharajan Engineering College.

REFERENCES

[1] H.S. Nalwa, S. Miyata, *Nonlinear Optics of Organic Molecules and Polymer*.
[2] P.N. Prasad, D.J. Williams, *Introduction to Nonlinear Optical Effects in Organic Molecules and Polymer*.
[3] S. Brahadeeswaran, V. Venkataramanan, J.N. Sherwood, H.L. Bhat, J. Mater. Chem **8**(3) (1998) 613–618.
[4] S. Brahadeeswaran, V. Venkataramanan, H.L. Bhat, J. Cryst. Growth **205** (1999) 548–553.
[5] S. Brahadeeswaran, Y. Takahashi, M. Yoshimura, M. Tani, S. Okada, S. Nashima, Y. Mori, M. Hangyo, H. Ito, T. Sasaki, Crys. Growth Des. **13** (2013) 415–421.
[6] B.M. Boaz, M. Palanichamy, B. Varghese, C.J. Raj, S.J. Das. Mater. Res. Bull **43**(2008) 3587–3595.
[7] B.M. Boaz, A.L. Rajesh, S.X.J. Raja, S.J. Das, J. Cryst. Growth **262** (2004) 531–535
[8] A.J. Varjula, C. Vesta, C.J. Raj, S. Dinakaran, A. Ramanand, S.J. Das. Mater.Lett. **61** (2007) 5053–5055.
[9] C. Vesta, R. Uthrakumar, B. Varghese, S.M.N. Priya, S.J. Das. J. Cryst. Growth **311**(2009) 1516–1520.
[10] P. Srinivasan, Y. Vidyalakshmi, R. Gopalakrishnan, Cryst. Growth Des. **8**(2008)2329–2334.